Equilibrium properties of a bidisperse ferrofluid with chain aggregates: theory and computer simulations

2006 J. Phys.: Condens. Matter 18 S2737

(http://iopscience.iop.org/0953-8984/18/38/S14)

INSTITUTE OF PHYSICS PUBLISHING JOURNAL OF PHYSICS: CONDENSED MATTER

J. Phys.: Condens. Matter **18** (2006) S2737–S2756 doi:10.1088/0953-8984/18/38/S14

Equilibrium properties of a bidisperse ferrofluid with chain aggregates: theory and computer simulations

Christian Holm[1,2], **Alexey Ivanov**[3], **Sofia Kantorovich**[2,3], **Elena Pyanzina**[3] **and Evgeniy Reznikov**[1,2,3]

[1] Frankurt Institute for Advanced Studies, J W Goethe-Universität, Max-von-Laue Straße 1, D-60438, Frankfurt/Main, Germany
[2] Max-Planck-Institut für Polymerforschung, Ackermannweg 10, D-55128, Mainz, Germany
[3] Department of Mathematical Physics, The Urals State University, 51 Lenin Avenue, Ekaterinburg 620083, Russia

E-mail: c.holm@fias.uni-frankfurt.de, alexey.ivanov@usu.ru, sue.kantorovich@usu.ru, snegn_bars@mail.ru and reznikov@fias.uni-frankfurt.de

Received 1 May 2006, in final form 19 June 2006
Published 8 September 2006
Online at stacks.iop.org/JPhysCM/18/S2737

Abstract

In this paper we investigate a bidisperse model ferrofluid, where the aggregates are treated as flexible chains, under the influence of an arbitrary valued external magnetic field. An extensive comparison of the theoretical predictions to the results of the computer simulations is provided. Both magnetostatic properties and structural observables are investigated with the help of the newly developed theoretical approach and molecular dynamic simulations. It is shown that the results of the cluster analysis are very sensitive to the cluster definition. Here we use two different criteria for the particles to be bound: an *energy* criterion which is slightly different in the theory and simulations due to technical problems, and an *entropy* criterion which is the same for the molecular dynamics and theoretical model. This enables us to compare qualitatively and quantitatively theoretical and numerical microstructural observables, as well as the macro properties of the bidisperse ferrofluids. Finally, an answer to the question which chain criterion should actually be used is provided in this paper.

1. Introduction

First synthesized in the beginning of the 1960s [1], magnetic fluids (known also as ferrofluids or ferrocolloids) consisting of single-domain ferro- (ferri-, antiferro-) magnetic particles in a magnetopassive liquid environment appeared to be an excellent example of magnetocontrollable systems. These particles in ferrocolloids (usually made of Co, Fe, Ni and their oxides) have a size of less than 25–30 nm, which is why they experience only a very weak concentration gradient in the gravitational field and almost never sediment. To avoid irreversible aggregation in a system, particles are stabilized by steric coatings (in nonelectrolytic carrier liquids) or by electrical double layers (in aqueous solutions). Their unique combination of strong response to

an external magnetic field together with their liquid state gives rise to numerous applications of magnetic fluids in engineering and arts, and magnetic fluids also appear to be very useful in biomedical applications, such as an effective tool in cancer treatment [2, 3].

The first theoretical models treated the ferrofluid as an ideal superparamagnetic gas [4], in which the magnetization obeys a Langevin law. However, experimental evidence demonstrated clearly that the magnetic particle did interact. An attempt to apply the Ising model and directly introduce a molecular Weiss field gave good results for ferrofluids with a low magnetic concentration and high fields [5] but was not quite as successful in other cases. This is because, unlike the exchange interaction with a constant sign, the noncentral magnetic dipole–dipole interparticle interaction can change sign from attraction to repulsion. Thus, the spontaneous magnetization predicted by the Weiss model is improbable in ferrocolloids, and has never been observed in any experiment. The so-called modified mean field approach [6, 7] and the first-order perturbation theory [8] allowed the development of a theoretical ferrofluid model with interparticle interactions taken into account. However, detailed experimental analysis of magneto-optic [9–11], magneto-viscous [12–14] and diffusion [15] properties of ferrofluids very soon hinted towards the existence of a complex anisotropy in the ferrofluid microstructure in an external magnetic field. The reason for this anisotropy was the presence of different aggregates, which were attributed to the following structures: chain aggregates (tens of nanometres in size), fractal loose aggregates (hundreds of nanometres in size) and drops (micrometres in size). A number of various computer simulations were used to analyse the microstructure of a ferrofluid [16–20]. All of these works reported the presence of linear chain-like structures in the systems investigated. Recently these observations found an experimental proof in cryo-TEM microscopy [21]. The theoretical description of chaining is usually based on the density functional approach [22–24]. Unfortunately, until recently, almost all known theoretical studies dealt with model monodisperse dipolar fluids and magnetic colloids. This was mostly caused by the mathematical difficulties encountered in building the partition function for the multicomponent system with non-central magnetic interaction (either in terms of hard sphere repulsion or Lennard-Jones interaction). The next approximation that was usually adopted in these theories is related to the chain rigidity, i.e. chains were considered to be rod-like structures. Such an approximation might be valid only for highly interacting particles. The other problem is that the influence of an external magnetic field was taken into account only in the region of the magnetic saturation, where the magnetic moment of each particle was aligned with the magnetic field. This was done since it resulted in a nice factorization of the partition function for each chain.

In the present paper we get rid of the major part of these approximations, namely we treat a bidisperse model ferrofluid with flexible chains under the influence of an arbitrary valued external magnetic field. Such a system was recently studied by one of us in computer simulations [16]. In this work we provide an extensive comparison of the theoretical predictions to the results of the computer simulations. In the next section we will describe the details of our computer model. In section 3 we compare the newly developed theoretical approach with the results of the molecular dynamic simulations on the magnetostatic properties. It turns out that with the energy criterion for the theoretical cluster definition we can easily reach a nice accord between theoretically and numerically predicted magnetization curves and initial susceptibility for different granulometric compositions of our model fluid. However, a more detailed analysis of the cluster structure shows noticeable deviations in cluster sizes and distributions when compared to the simulational results. This happens partially because a different energy cluster criterion for the cluster analysis is used in simulation. Due to technical problems we simply cannot use exactly the same *energy* criterion in the theoretical analysis and in the simulations. In section 4 we prove that the observed differences in the structural analysis is caused exactly by the difference between cluster definitions. For this we perform an extensive theoretical and

numerical cluster analysis with the same, now *entropic*, cluster definition. This enables us to compare qualitatively and quantitatively theoretical and numerical microstructural observables. Physical results of the work and the scope of different cluster definitions, for example, which chain criterion should actually be used, are discussed in the conclusions, which are found in section 5. From the investigations carried out in sections 2–4 one can easily understand that the nearest neighbour limitation and the neglect of interchain interaction, which are still present in the theory, are compensating each other. Our presented newly developed theoretical approach might be used to describe the ferrofluid macroscopic properties and their microstructure.

2. Bidisperse model: computer simulations

The investigated ferrofluid systems consist of N spherical particles distributed in a cubic simulation box of side length L. Each particle has a diameter of σ_i and a permanent point dipole moment $\mathbf{m}_i$ at its centre. The dipole–dipole interaction potential between particle i and j is given by

$$U_d(ij) = -\frac{\mu_0}{4\pi}\left[3\frac{\langle \mathbf{m}_i, \mathbf{r}_{ij}\rangle\langle \mathbf{m}_j, \mathbf{r}_{ij}\rangle}{r^5} - \frac{\langle \mathbf{m}_i, \mathbf{m}_j\rangle}{r^3}\right], \qquad \mathbf{r}_{ij} = \mathbf{r}_i - \mathbf{r}_j \tag{1}$$

where $\mathbf{r}_{ij}$ is the displacement vector of the two particles and $\mu_0 = 4\pi \times 10^{-7}$ H m^{-1} is the vacuum magnetic permeability. Using periodic boundary conditions in all spatial directions, the dipole–dipole interaction is evaluated by the Ewald summation under metallic boundary condition, which gives [25, 26]

$$U_d(ij) = -\langle \mathbf{m}_i, \bigtriangledown\rangle\langle \mathbf{m}_j, \bigtriangledown\rangle\Psi(\mathbf{r}_{ij}), \tag{2}$$

with

$$\Psi(\mathbf{r}) = \frac{\mu_0}{4\pi}\left[\sum_{\mathbf{n}\in Z^3}\frac{\operatorname{erfc}(\kappa|\mathbf{r}+\mathbf{n}L|)}{|\mathbf{r}+\mathbf{n}L|} + \frac{1}{\pi L}\sum_{n\neq 0} n^{-2}\exp\left(\frac{-\pi^2 n^2}{\kappa^2 L^2} + \frac{2\pi \mathrm{i}}{L}\langle \mathbf{n}, \mathbf{r}\rangle\right)\right]. \tag{3}$$

Here the sum in equation (3) is performed in a spherical fashion and extends over all simple cubic lattice points $\mathbf{n} = (k, l, m)$ with k, l, m integers, and $\operatorname{erfc}(x)$ denotes the complementary error function. The inverse length κ is the splitting parameter of the Ewald sum which weights the relative contribution of the real and Fourier space parts. The use of the metallic boundary condition means that no demagnetization effects occur and the applied external magnetic field coincides exactly with the internal field [25–28]. The related formulae for the dipolar force $\mathbf{F}_{ij}^{\mathrm{dip}}$ and torque $\boldsymbol{\tau}_{ij}^{\mathrm{dip}}$ can be found in [27], where theoretical estimates of the cutoff errors in the Ewald summation were derived. They were used to determine the optimal values for the Ewald parameters, thereby enabling us to minimize the overall computational time at a predefined accuracy.

The short-range interactions between the particles are represented by a purely repulsive Lennard-Jones potential. Considering the different sizes of the particles, this potential is written as

$$U_{\mathrm{LJ}}(ij) = 4\epsilon\left[\left(\frac{\sigma_i + \sigma_j}{2r_{ij}}\right)^{12} - \left(\frac{\sigma_i + \sigma_j}{2r_{ij}}\right)^{6}\right] + \epsilon, \tag{4}$$

with a cutoff radius of $R_{\mathrm{c}} = 2^{-5/6}(\sigma_i + \sigma_j)$. In this way the particles have a purely repulsive force which smoothly decays to zero at R_{c}. The molecular dynamics simulation method is the same as the Langevin dynamics implementation described in [27]. For simulating polydisperse systems, the size variables can be defined according to a reference diameter that is normally taken to be the mean size of the particles. In our bidisperse case, we take σ_{s} to be the diameter of the small particles. We use reduced variables such as a constant reduced temperature

$T^* = kT/\epsilon = 1$, and a reduced time $t^* = t(\epsilon/m_0\sigma_s^2)^{1/2}$, employing a reduced time step of $\Delta t^* = 2$–3×10^{-3}. The accuracy of the Ewald sum was tuned to an absolute root mean square error in the dipolar forces of $\Delta F^{\mathrm{dip}} \leqslant 10^{-4}\mu_0 m_0^2/4\pi\sigma_s^4$. The runs were started from initial configurations with random particle positions and dipole moment orientations. The equilibration time was found to be about $t^* = 100$ for the monodisperse system of small particles, which could go up to $t^* = 500$ for systems with a high fraction of large particles. The total simulation time was at least 3–4 times longer than the equilibration time. Error bars for the simulation results were determined by dividing the simulation runs into blocks and calculating an estimate for the standard deviation of the mean. More simulation details can be found in [16, 29].

Our bidisperse ferrofluid system consists of two fractions of magnetite particles with saturation magnetization of the material M_{m} equal to 4.8×10^5 A m^{-1}. The diameter of small fraction particles σ_{s} is taken to be 10 nm, and for the diameter of the large particles we used $\sigma_{\mathrm{l}} = 16$ nm. Particle magnetic moments are $m_i = \pi\sigma_i^3 M_{\mathrm{m}}/6$, where the index i might have two different values: $i \in \{\mathrm{s}, \mathrm{l}\}$ for small and large particles respectively. So, three different dipolar coupling constant could be calculated: for the interaction between two large particles (two small particles) we obtain $\lambda_{\mathrm{ll(ss)}} = \mu_0 m_{\mathrm{l(s)}}^2/4\pi kT\sigma_{\mathrm{l(s)}}^3$; for the interaction between small and large particle the expression for this parameter could be written in a form $\lambda_{\mathrm{sl}} = 2\mu_0 m_{\mathrm{s}} m_{\mathrm{l}}/\pi kT(\sigma_{\mathrm{s}} + \sigma_{\mathrm{l}})^3$. At room temperature, $T = 300$ K, these values are found to be $\lambda_{\mathrm{ll}} = 5.32$, $\lambda_{\mathrm{ss}} = 1.3$, $\lambda_{\mathrm{sl}} = 2.42$.

Two different cases are studied in the present paper. In the first case the total volume fraction of particles ϕ is fixed to the value of 0.07, which is typical for normal commercial ferrofluids. In order to study the influence of polydispersity on the static magnetic properties the volume fraction of large particle, ϕ_{l}, could be varied. In our case the following values of ϕ_{l} are investigated: $\phi_{\mathrm{l}} = 0$; 0.007; 0.02; 0.05; 0.07. Thus we go from a monodisperse system consisting of small particles only through the bidisperse cases, and finally to a monodisperse system composed purely by large particles. The total number N of particles in the simulation box is mainly taken to be $N = 1000$. But a much larger number of N (=3029) is used in the case of $\phi_{\mathrm{l}} = 0.007$ in order to enhance the statistics with a sufficient number of large particles.

In the second case we analyse the influence of small particles on the cluster structure. Here the large particle volume fraction is fixed to $\phi_{\mathrm{l}} = 0.05$ and the volume fraction of small particles is varied from $\phi_{\mathrm{s}} = 0$ to 0.05. The number of large particles is taken to be $N_{\mathrm{L}} = 500$. The total number of particles is increased from $N = 500$ to 2548.

The cluster analysis in the simulation is based on an *energy simulation criterion*: two particles are considered to be bound if the absolute value of their dipolar interaction is larger than 70% of the contact energy of two perfectly coaligned dipolar particles.

First of all the analysis of the magnetization curves for the fluids with different large particle concentrations and their initial susceptibility was carried out. The influence of the external magnetic field H is introduced in a form of dimensionless Langevin parameters for both fractions, which are given by

$$\alpha_{\mathrm{s}}(H) = \mu_0 m_{\mathrm{s}} H/kT, \qquad \alpha_{\mathrm{l}}(H) = \mu_0 m_{\mathrm{l}} H/kT.$$

The analysis showed the strong dependence of the magnetization on the concentration of large particles at low fields. Thus, when the concentration of large particles is small, the magnetization behavior is close to the one given by the modified mean field approach for homogeneous ferrofluids [6, 7]:

$$\begin{aligned} &M_{\mathrm{mf}}(H) = M_{\mathrm{L}}[H_e(H)], \\ &\chi_{\mathrm{mf}} = \left.\frac{\partial M_{\mathrm{mf}}(H)}{\partial H}\right|_{H=0}, \qquad H_e(H) = H + \tfrac{1}{3}M_{\mathrm{L}}(H), \\ &M_{\mathrm{L}}(H) = \left[\rho_{\mathrm{s}}/v_{\mathrm{s}}\right] L[\alpha_{\mathrm{s}}(H)] + \left[\rho_{\mathrm{l}}/v_{\mathrm{l}}\right] L[\alpha_{\mathrm{l}}(H)], \end{aligned} \tag{5}$$

where $L(x)$ denotes the Langevin function, and v_s, v_l, ρ_s, ρ_l are the small and the large fraction particle volumes and volume concentrations, respectively. This means that $M_L(H)$ is the Langevin magnetization for a bidisperse model. This approach [6, 7] allows us to take into account the influence of interparticle interactions between all particles in a system on the magnetization. The additional term in the expression for H_e follows from the first-order perturbation theory and does not depend on the short-range correlations in a system; in other words, $1/3M_L(H)$ might be obtained by expanding the free energy into a virial series for low concentrated ferrofluids. The modified mean field approach has proved to describe magnetic properties of moderately concentrated ferrocolloids very accurately. Here the value χ_{mf} stands for the initial susceptibility of the bidisperse ferrofluid in terms of the modified mean field approach. The higher the portion of large particles is, the more noticeable is the growth of the initial susceptibility. The cluster analysis evidences that the aggregation behaviour becomes evident when $\phi_l = 0.05$, and as soon as the system consists of large particles only long chains (3–5 particles) might be observed. The aggregates with uncompensated magnetic moments are supposed to react on the fields weaker than the one that single particles react on, which is why the presence of such aggregates leads to an increase of the initial susceptibility. So, in order to describe the static magnetic properties of systems with a considerable concentration of large particles, it is absolutely essential to develop a new approach that allows for the presence of chains.

3. Bidisperse model: theory, energy criterion

The static magnetic properties are studied here on the basis of the free energy density functional approach. Chains could be composed by particles from both fractions and the equilibrium volume concentration of chains formed by n large particles and m small particles with topology i in an arbitrary external magnetic field H is $g(i, n, m, H)$ (for details, see [30]). The volume of such chains $v(i, n, m)$ depends on the topological alignment of particles, i.e. on the values of a, b, c which stand for the number of small–small particle, large–small particle, and large–large particle bonds in a chain respectively:

$$v(i, n, m) = v_s^{-a} v_{sl}^{m-b} v_l^{n-c}, \qquad a + b + c = n + m - 1.$$

Since the interaction energy between two small particles in our investigated system is extremely low, we omit all chains in which two small particles are neighbours; hence $a = 0$. In order to obtain the free energy density one has to sum up the energies of the chains for every value of n, m and arbitrary topology. The topological summation has to be carried out until the total number $I(n, m)$ of energetically different chains for every pair m, n is taken into account. However, for the fixed n, m there are chains having the same energy, but different topology. To take this into account, the entropic factor $K(i, n, m)$, which is equal to the number of entropically distinguishable chains with the same energy, is used.

For a bifractional system the following free energy functional appears as a natural generalization of Frenkel's thermal fluctuations theory [31] and the bidisperse model developed in [30]:

$$\begin{aligned} F(H) &= F_s(H) + F_l(H) + kT \sum_{n+m\geqslant 1}^{\infty} \sum_{i=1}^{I(n,m)} K(i, n, m) g(i, n, m, H) \\ &\quad \times \left[\ln \frac{g(i, n, m, H) v(i, n, m)}{e} - \ln Q(i, n, m, H) \right], \\ F_{s(l)}(H) &= -kT \left[\rho_{s(l)} / v_{s(l)} \right] \ln \left[\sinh(\alpha_{s(l)}(H)) / \alpha_{s(l)}(H) \right], \end{aligned} \tag{6}$$

where expressions for $F_s(H)$ and $F_l(H)$ reflect the field response of small and large particles regardless of whether they are members of a chain or not. Within this paper we use a special way of bracketing to simplify mathematical expressions: when written $F_{s(l)}(H)$ this means that

two expressions for small particles $F_{\rm s}(H)$ and large particles $F_{\rm l}(H)$ have the same form and differ only in the indices of the variables appearing in them (in equation (6), the difference lies in volumes $v_{\rm s}$, $v_{\rm l}$ in particular). The key feature of the functional (6) is hidden in a chain partition function $Q(i, n, m, H)$, whose evaluation has long been a stumbling block for theorists. To calculate the chain partition function one has to introduce the chain definition. Here we use the bidisperse generalization of the approach developed in [32], where the analytical form for a chain partition function has been obtained for the monodisperse case.

The *theoretical cluster criterion* which is used here is the following. Two particles i and j are considered to be bound if the values of differences

$$\frac{\langle \mathbf{m}_i, \mathbf{m}_j \rangle}{|\mathbf{m}_i||\mathbf{m}_j|} - 1, \qquad \frac{\langle \mathbf{m}_i, \mathbf{r}_{ij} \rangle}{|\mathbf{m}_i||\mathbf{r}_{ij}|} - 1, \qquad \frac{\langle \mathbf{m}_j, \mathbf{r}_{ij} \rangle}{|\mathbf{m}_j||\mathbf{r}_{ij}|} - 1$$

are infinitesimals of the second order. In other words two particles are bound if their magnetic moments are almost coaligned, and both magnetic moments are almost coaligned with the radius vector. The coupling energy between two bounded particles has to be larger than 2.

Unlike the *energy simulation criterion*, in which no particular spatial alignment of particles is demanded, here we have visible restrictions for the magnetic moments and radius vectors.

So, the expression for $Q(i, n, m, H)$, as a bidisperse extension of the partition function calculated in [32], has the following form:

$$Q(i, n, m, H) = q_\infty(\mathrm{ll})^c q_\infty(\mathrm{sl})^b D(i, n+m, H) \prod_{j=1}^{n+m-1} C(i, j, H), \tag{7}$$

where $Q(i, 1, 0, H) = Q(i, 0, 1, H) = 1$.

$$D(i, n+m, H) = \begin{cases} \dfrac{\sinh[\alpha_{\rm s}(H) f^1_{n+m}]}{\sinh[\alpha_{\rm s}(H)] f^1_{n+m}}, & \text{if } n+m \text{ particle is small;} \\ \dfrac{\sinh\left[\alpha_{\rm l}(H) f^{2(3)}_{n+m}\right]}{\sinh[\alpha_{\rm l}(H)] f^{2(3)}_{n+m}}, & \text{if } n+m \text{ particle is large.} \end{cases}$$

$$C(i, j, H) = \begin{cases} \dfrac{\alpha_{\rm l}(H)}{\sinh[\alpha_{\rm l}(H)]} \dfrac{\sinh\left[\alpha_{\rm l}(H) f^{2(3)}_j + a^1_{jj+1}\right]}{\alpha_{\rm l}(H) f^{2(3)}_j + a^1_{jj+1}} \\ \qquad \times \exp\left[-a^1_{jj+1} \left\{ 1 + \alpha_{\rm l}(H) \dfrac{f^{2(3)}_j L\left[\alpha_{\rm l}(H) f^{2(3)}_j + a^1_{jj+1}\right]}{\alpha_{\rm l}(H) f^{2(3)}_j + a^1_{jj+1}} \right\} \right], \\ \qquad \text{if } j \text{ particle is large and } j+1 \text{ particle is small;} \\ \dfrac{\alpha_{\rm l}(H)}{\sinh[\alpha_{\rm l}(H)]} \dfrac{\sinh\left[\alpha_{\rm l}(H) f^{2(3)}_j + a^2_{jj+1}\right]}{\alpha_{\rm l}(H) f^{2(3)}_j + a^2_{jj+1}} \\ \qquad \times \exp\left[-a^2_{jj+1} \left\{ 1 + \alpha_{\rm l}(H) \dfrac{f^{2(3)}_j L\left(\alpha_{\rm l}(H) f^{2(3)}_j + a^2_{jj+1}\right)}{\alpha_{\rm l}(H) f^{2(3)}_j + a^2_{jj+1}} \right\} \right], \\ \qquad \text{if } j \text{ particle is large and } j+1 \text{ particle is large;} \\ \dfrac{\alpha_{\rm s}(H)}{\sinh[\alpha_{\rm s}(H)]} \dfrac{\sinh\left[\alpha_{\rm s}(H) f^1_j + a^1_{jj+1}\right]}{\alpha_{\rm s}(H) f^1_j + a^1_{jj+1}} \\ \qquad \times \exp\left[-a^1_{jj+1} \left\{ 1 + \alpha_{\rm s}(H) \dfrac{f^1_j L\left(\alpha_{\rm s}(H) f^1_j + a^1_{jj+1}\right)}{\alpha_{\rm s}(H) f^{2(3)}_j + a^1_{jj+1}} \right\} \right], \\ \qquad \text{if } j \text{ particle is small and } j+1 \text{ particle is large.} \end{cases}$$

Here the coefficients $f_{j+1}^{1(2,3)}$ have the following recursive definition:

$$f_{j+1}^{1} = 1 + \frac{\alpha_{\mathrm{l}}(H)}{\alpha_{\mathrm{s}}(H)} \frac{a_{jj+1}^{1} f_{j}^{2(3)} L\left[\alpha_{\mathrm{l}}(H) f_{j}^{2(3)} + a_{jj+1}^{1}\right]}{\alpha_{\mathrm{l}}(H) f_{j}^{2(3)} + a_{jj+1}^{1}},$$

if $j+1$ particle is small and j particle is large;

$$f_{j+1}^{2} = 1 + \frac{\alpha_{\mathrm{l}}(H)}{\alpha_{\mathrm{l}}(H)} \frac{a_{jj+1}^{2} f_{j}^{2(3)} L\left[\alpha_{\mathrm{l}}(H) f_{j}^{2(3)} + a_{jj+1}^{2}\right]}{\alpha_{\mathrm{l}}(H) f_{j}^{2(3)} + a_{jj+1}^{2}},$$

if $j+1$ particle is large and j particle is large;

$$f_{j+1}^{3} = 1 + \frac{\alpha_{\mathrm{s}}(H)}{\alpha_{\mathrm{l}}(H)} \frac{a_{jj+1}^{1} f_{j}^{1} L\left[\alpha_{\mathrm{s}}(H) f_{j}^{1} + a_{jj+1}^{1}\right]}{\alpha_{\mathrm{s}}(H) f_{j}^{1} + a_{jj+1}^{1}},$$

if $j+1$ particle is large and j particle is small.

The first coefficient in the set is equal to unity $f_1^s = 1$ for $s = 1, 2, 3$. The factors $a_{ii+1}^{1(2)}$ could be found from the following equations:

$$\int \frac{\mathrm{d}\mathbf{r}_{ii+1}}{v_{\mathrm{sl(l)}}} \exp\left[-\frac{U_d(ii+1) + U_{\mathrm{LJ}}(ii+1)}{kT}\right] = q_\infty(ii+1) \exp\left[a_{ii+1}^{1(2)} (\cos\omega_{i+1} - 1)\right], \qquad \exp(2\lambda_{ii+1}) \gg 1; \tag{8}$$

$$q_\infty(ii+1) = \int \frac{\mathrm{d}\mathbf{r}_{ii+1}}{v_{\mathrm{ll(sl)}}} \exp\left[-\frac{U_d(ii+1) + U_{\mathrm{LJ}}(ii+1)}{kT}\right],$$

where ω_{i+1} stands for the angle between the direction of an external magnetic field and the magnetic moment of the particle with number $i+1$ in the standard spherical coordinate system [33]. The theoretical criterion defined above restricts the integration limits in expression (8). The distance between two particles $(i, i+1)$ in a chain cannot exceed a certain value. This distance is to be chosen from the condition that for the coupling energy less than 2 ($\lambda_{ii+1} < 2, i, i+1 \in \{\mathrm{s}, \mathrm{l}\}$), chains are not stable. This energy limitation is based on the results of computer simulations [17], where no chaining is observed for systems with coupling energy less than 2. With the increase of the distance between particles the characteristic coupling energy decreases as λ_{ii+1}/z_{ii+1}, where $z_{ii+1} = 8r_{ii+1}^3/(\sigma_i + \sigma_{i+1})^3$. So, the critical value of z_{ii+1}^c (the largest allowable distance) is $z_{ii+1}^c = \lambda_{ii+1}/2$. For such an upper limit in (8), using the saddle point technique [32], the integrals should be rewritten:

$$\frac{2}{3\lambda_{ii+1}} \int_0^{z_{ii+1}^c} z_{ii+1} \exp\left[-\frac{U_{\mathrm{LJ}}(ii+1)}{kT}\right] \exp\left[\frac{2\lambda_{ii+1}}{z_{ii+1}}\right] \exp\left[\frac{\lambda_{ii+1}}{2z_{ii+1}} (\cos\omega_{i+1} - 1)\right] \mathrm{d}z_{ii+1} = \exp\left[a_{ii+1}^{1(2)} (\cos\omega_{i+1} - 1)\right] \frac{2}{3\lambda_{ii+1}} \int_0^{z_{ii+1}^c} z_{ii+1} \exp\left[-\frac{U_{\mathrm{LJ}}(ii+1)}{kT}\right] \times \exp\left[\frac{2\lambda_{ii+1}}{z_{ii+1}}\right] \mathrm{d}z_{ii+1}. \tag{9}$$

Finally, the free energy (6) minimum has to be found under the mass balance conditions:

$$\frac{\rho_{\mathrm{s}}}{v_{\mathrm{s}}} = \sum_{n+m\geqslant 1}^{\infty} \sum_{i=1}^{I(n,m)} K(i,n,m) g(i,n,m,H) m, \tag{10}$$

$$\frac{\rho_{\mathrm{l}}}{v_{\mathrm{l}}} = \sum_{n+m\geqslant 1}^{\infty} \sum_{i=1}^{I(n,m)} K(i,n,m) g(i,n,m,H) n. \tag{11}$$

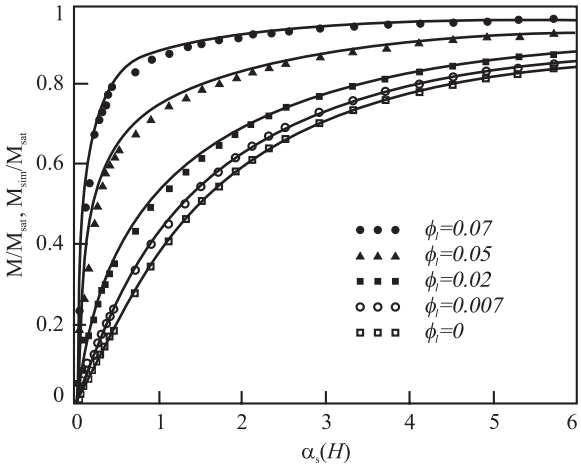

Figure 1. Magnetization related to the saturation magnetization (M_s) versus small particle Langevin parameter $\alpha_s(H)$ for different volume fractions of large particles ϕ_l. Here computer simulation data M_{sim}/M_s are given as symbols, and the theoretical predictions (6)–(13) M/M_s are presented in solid lines. The total particle volume fraction ϕ is fixed at 0.07.

Using Lagrange's method we obtain the solution

$$g(i,n,m,H) = p_s^m(H)\,p_l^n(H)\,Q(i,n,m,H)/v(i,n,m), \tag{12}$$

where p_s, p_l are the Lagrange multipliers to be calculated from equations (10) to (11).

As soon as the free energy of the system in thermodynamic equilibrium is known it is quite easy to calculate both the static magnetization and the initial susceptibility. We stress that it is not an external field H that acts on each particle in a system, but the effective field H_e from equation (5). It is worth saying, that the chain's presence does not lead to any changes in the expression for the effective field, because in the form given by equation (5) it is independent of the type of short-range interparticle interactions which are responsible for the chaining in a system. So, finally, the following expressions could be written for static magnetization $M(H)$ and initial susceptibility χ for a bidisperse ferrofluid with chain aggregates:

$$M(H) = -\frac{\partial F(H)}{\partial H}\bigg|_{H=H_e}; \qquad \chi = \frac{\partial M(H)}{\partial H}\bigg|_{H=0}. \tag{13}$$

Here, following the mean field approach, the magnetization of the system depends on H_e. This replacement was used before for a monodisperse case [34] and appeared to be a very good approximation. In order to check the developed theoretical model a comparison between simulation data and theoretical predictions (6)–(13) is carried out.

Five different samples with total volume fraction of particles fixed at $\phi = 0.07$ are investigated. We used the volume fraction of large particles $\phi_l = 0$; 0.007; 0.02; 0.05; 0.07. For the monodisperse system of small particles, both the modified mean field theory and the chain model give results very close to the numerical data. The ratio of the magnetization to the saturation magnetization M_s is plotted versus small particle Langevin parameter α_s in figure 1 (computer simulation data M_{sim}/M_s are given in symbols, theoretical predictions (6)–(13) M/M_s are presented in solid lines) for $\phi_l = 0.007$, 0.02, 0.05, 0.07. The comparison between simulation results (dots) and theoretical model (13) (solid line) for the initial susceptibility χ as a function of large particle volume fraction ϕ_l is presented in figure 2. As can be clearly seen, the results of the theoretical model (6)–(13) are close to the simulation dots. However, the

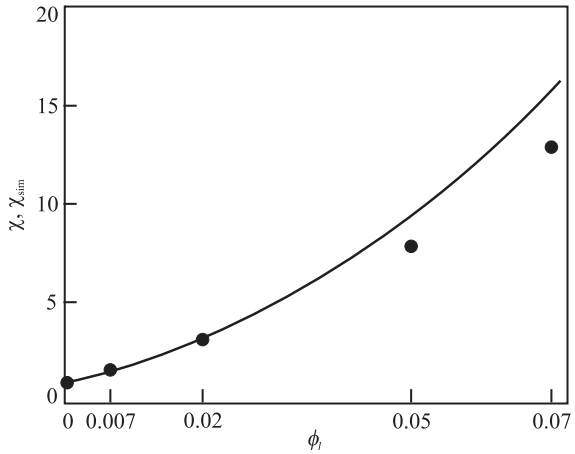

Figure 2. Initial susceptibility χ as a function of large particle volume fraction ϕ_l. The theoretical prediction (equation (13)) is plotted as a solid line, and numerical results are given as dots (χ_{sim}). The total particle volume fraction ϕ is fixed at 0.07.

developed approach overestimates the initial susceptibility, and the deviations grow when the large particle volume fraction increases. To analyse the reason for these deviations the cluster analysis is provided.

Here we investigated the average chain length and cluster distributions for different bidisperse systems. The average cluster size is defined by the expression

$$N(H, \phi_l, \phi_s) = \frac{\sum_{n+m\geqslant 1}^{\infty} \sum_{i=1}^{I(n,m)} n g(i, n, m, H)}{\sum_{n+m\geqslant 1}^{\infty} \sum_{i=1}^{I(n,m)} g(i, n, m, H)}. \tag{14}$$

This means that the average number of large particles per chain is calculated. According to the theoretical predictions for the maximal external magnetic field strength this value reaches $N(H_{max}, 0.07, 0) = 7.7$, $H_{max} \sim 90$ kA m^{-1} when the large particle volume fraction equals $\phi_l = 0.07$. The calculation of the same quantity in computer simulation gives a value which appears to be much lower, that is $N(H_{max}, 0.07, 0) = 4.5$. Deviations of this order are observed between theory and simulations for any granulometric composition and for any value of an external magnetic field. In other words, the theoretical approach does overestimate the chain length. This fact might explain the discrepancies in the numerically obtained and theoretically predicted initial susceptibility. However, the main reason for such a difference in cluster analysis might be treated in several ways. On the one hand, the proposed theoretical model neglects interchain interactions which would lead to chain shortening. On the other hand, only the interaction between nearest neighbours is considered, while in the computer simulations all short- and long-range correlations are taken into account. It is worth mentioning that analytical estimates suggest that the chain growth due to the additional consideration of the next-nearest neighbour interactions is negligible. The discrepancy in quantitative microstructure observables might also be caused by the difference in the theoretical and simulation cluster definition. In order to bring the main reason of the deviations in cluster analysis to light we analyse the tendencies of cluster evolution for different granulometric compositions. The relative chain growth as a function of large particle concentration is presented in figure 3. Here the ratio $N(0, \phi_l, 0.07 - \phi_l)/N(0, 0.07, 0)$ is plotted as a function of large particle concentration in a zero external field for the fixed total concentration $\phi = 0.07$. Here and in subsequent figures dots correspond to the simulation data, and solid curves describe theoretical

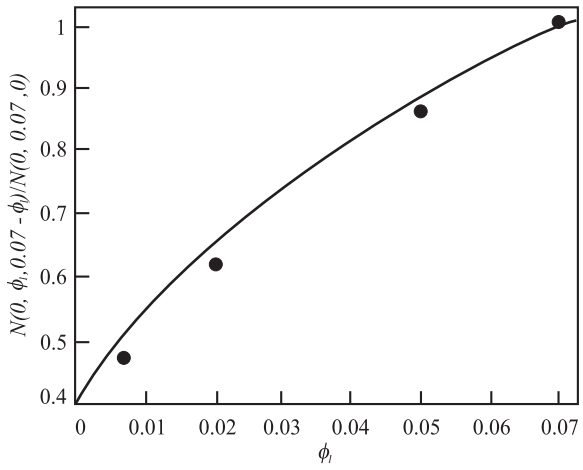

Figure 3. The relative chain growth $N(0, \phi_l, 0.07-\phi_l)/N(0, 0.07, 0)$ as a function of large particle concentration ϕ_l in zero external field. The total particle volume fraction ϕ is fixed at 0.07. The solid line describes the theoretical prediction, and simulation data are plotted as dots.

results. As is seen, the qualitative behaviour predicted by the above-mentioned theoretical model is similar to the one in the computer simulations. In other words, when the large particle concentration increases so that we start with model monodisperse system of small particles and through bidisperse systems come to a monodisperse large particle ferrofluid, the mean chain length increases by approximately 50%. Theoretically obtained values are $N(0, 0.007, 0.063) = 1.6$, $N(0, 0.07, 0) = 4.0$; the same values in the computer simulations appear to be relatively twice as small: $N(0, 0.007, 0.063) = 1.1$, $N(0, 0.07, 0) = 2.4$. The influence of an external magnetic field on the chaining for model binary mixtures with different granulometric composition is reflected by figure 4. In this figure the ratio $N(H, \phi_l, 0.07-\phi_l)/N(H_{max}, \phi_l, 0.07-\phi_l)$ is plotted for four different values of large particle concentration as a function of small particle Langevin parameter $\alpha_s(H)$. In figure 4(a) the system is composed by large particles only ($\phi_l = 0.07$); in figures 4(b)–(d) ϕ_l is equal to 0.05, 0.03, and 0.007 correspondingly. So, the less the large particle concentration is, the less is the relative field induced chain lengthening. For example, for the monodisperse system of large particles only the value of $N(H_{max}, 0.07, 0)$ in a strong field is almost twice as large than the one in a zero field (figure 4(a)). At the same moment the system in which the concentration of small particles is comparatively high (figure 4(d)) exhibits much lower aggregation tendency (some 25%) under the influence of an external magnetic field. The relative comparison between theory (curves) and simulations (dots) in figure 4 again gives us a very nice agreement. However, the characteristic difference between theoretically predicted and computationally obtained absolute values remains. Thus, as was mentioned above, the values of $N(H_{max}, 0.07, 0)$ differ by almost 50% in the theoretical model and computer simulations.

To analyse the influence of small particles on cluster sizes the total volume fraction of large particles is fixed at $\phi_l = 0.05$ and the small particle concentration is increased. In figure 5 the relative chain shortening $N(0, 0.05, \phi_s)/N(0, 0.05, 0)$ is presented. Here dots stand for the simulation results and the theoretically obtained 'poisoning effect' is illustrated by a solid line. It is clearly seen that the qualitative behaviour in the computer simulation and the theoretical model is the same: with an increase of small particle concentration the number of large particles per chain decreases by approximately 25%. The number of large particles per chain in theory

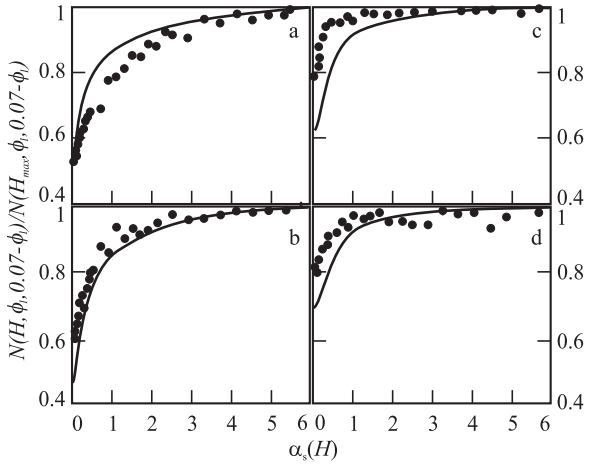

Figure 4. The ratio $N(H, \phi_l, 0.07 - \phi_l)/N(H_{max}, \phi_l, 0.07 - \phi_l)$ for four different values of large particle concentration as a function of small particle Langevin parameter $\alpha_s(H)$: $\phi_l = 0.07$ (a), 0.05 (b), 0.03 (c), 0.007 (d). The total particle volume fraction ϕ is fixed at 0.07. Solid lines correspond to theoretical results, and simulation data are plotted as dots.

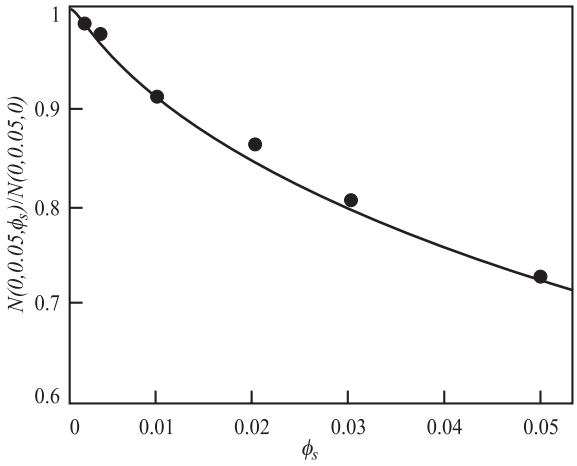

Figure 5. The relative chain shortening $N(0, 0.05, \phi_s)/N(0, 0.05, 0)$ as a function of small particle concentration. The volume fraction of large particles is fixed at $\phi_l = 0.05$. The theoretical result is plotted as a solid line, and the simulation data are given as dots.

decreases from $N(0, 0.05, 0) = 3.5$ to $N(0, 0.05, 0.05) = 3$ in comparison to the results of simulations which are the following: $N(0, 0.05, 0) = 2.5$ and $N(0, 0.05, 0.05) = 1.8$. The field influence might be studied by looking at figures 6 and 7, where field dependences of the relative average number of large and small particles per chain respectively are plotted versus small particle Langevin parameter $\alpha_s(H)$. Figure 6 allows us to analyse the influence of small particle concentration on the value of $N(H, 0.05, \phi_s)/N(H_{max}, 0.05, \phi_s)$. The relative field induced chain lengthening lies in between 30 and 50% for different small particle concentrations (in figure 6(a) $\phi_s = 0$, figure 6(b) $\phi_s = 0.01$, figure 6(c) $\phi_s = 0.03$, figure 6(d) $\phi_s = 0.05$). The average number of small particles per chain $N_s(H, \phi_l, \phi_s)$ has the

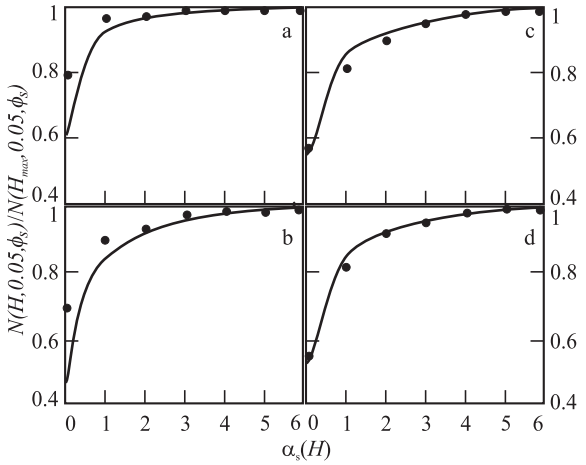

Figure 6. Field dependence of the relative average number of large particles per chain $N(H, 0.05, \phi_s)/N(H_{max}, 0.05, \phi_s)$ versus the small particle Langevin parameter $\alpha_s(H)$ for different small particle concentrations: $\phi_s = 0$ (a), 0.01 (b), 0.03 (c), 0.05 (d). The total volume fraction of large particles is fixed at $\phi_l = 0.05$. Theoretical results are presented by solid lines, and simulation data are plotted as dots.

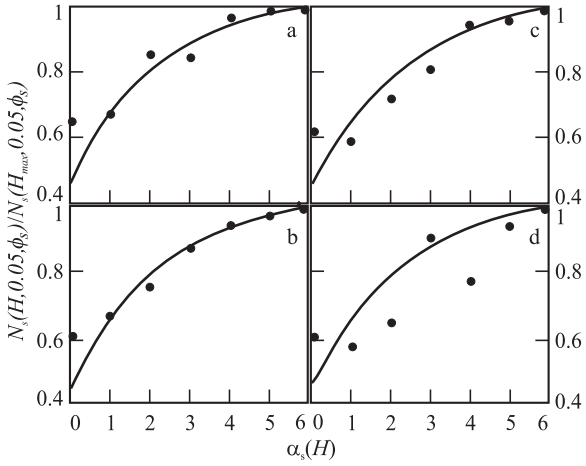

Figure 7. Field dependence of the relative average number of small particles per chain $N_s(H, 0.05, \phi_s)/N_s(H_{max}, 0.05, \phi_s)$ versus the small particle Langevin parameter $\alpha_s(H)$ for different small particle concentrations: $\phi_s = 0.05$ (a), 0.03 (b), 0.01 (c), 0.005 (d). The volume fraction of large particles is fixed at $\phi_l = 0.05$. Solid lines stand for theoretical results, and simulation data are given as dots.

following form:

$$N_s(H, \phi_l, \phi_s) = \frac{\sum_{n\geqslant 3, m>0}^{\infty} \sum_{i=1}^{I(n,m)} mg(i, n, m, H)}{\sum_{n\geqslant 3, m>0}^{\infty} \sum_{i=1}^{I(n,m)} g(i, n, m, H)}. \tag{15}$$

The summation in this expression is carried from $n = 3$; in other words, only aggregates with more than two large particles are allowed for. In figure 7(a) ($\phi_s = 0.05$), figure 7(b) ($\phi_s = 0.03$), figure 7(c) ($\phi_s = 0.01$), figure 7(d) ($\phi_s = 0.005$) the ratio $N_s(H, 0.05, \phi_s)/N_s(H_{max}, 0.05, \phi_s)$ is presented. These figures also reflect a perfect agreement

in qualitative behaviour between the theoretical model with the energy cluster definition and computer simulations. However, the absolute values do not match so nicely: the theoretically predicted average number of small particles per chain $N_s(H_{max}, 0.05, 0.05) = 0.48$ as opposed to the numerically obtained $N_s(H_{max}, 0.05, 0.05) = 0.38$.

Summing up the results of this section, our investigations showed that with the energy criterion for the theoretical cluster definition in demand a nice agreement between theoretically and numerically predicted magnetization curves and initial susceptibility for different granulometric compositions of a model fluid can be obtained. However, a more thorough analysis of the cluster structure reveals noticeable deviations in cluster sizes and distributions. Taking into account the total agreement between the simulation and the theoretical qualitative (relative) behaviour of different model binary ferrofluids which has just been shown for every microstructural observable, the following conclusion can be drawn. The deviations in cluster analysis between theory and computer simulations are not qualitative. In the next section we will actually demonstrate that they are caused by the difference in the cluster criterion. Unfortunately since neither can the theoretical energy criterion be applied to analyse the simulations, nor can the cluster definition of the simulations be used in the theoretical model directly, we will demonstrate the agreement by constructing a cluster criterion based on a pure geometric criterion, which we call henceforward *entropic*.

4. Bidisperse model: theory, entropy criterion

To prove that the differences in structure analysis is caused exactly by the gap between cluster definitions an *entropic* cluster definition is introduced in this section, which has the advantage that it can be used in the theory as well as in the simulations. Two particles $(i, i+1)$ are considered to be bound if the following relations hold true:

$$|\mathbf{r}_{ii+1}| \leqslant R_c(ii+1), \qquad \langle \mathbf{m}_i, \mathbf{m}_{i+1} \rangle \geqslant 0, \qquad \langle \mathbf{m}_i, \mathbf{r}_{ii+1} \rangle \langle \mathbf{m}_{i+1}, \mathbf{r}_{ii+1} \rangle \geqslant 0,$$

where $R_c(ii+1) = 2^{1/6} d_{ii+1}$ stands for the Lennard-Jones potential cutoff radius (see section 2). The second inequality means that the angle between neighbouring particle magnetic moments has to be equal to or less than 90°. The allowable region for the second particle is presented in figure 8(a). The third item forbids the artificial mutual alignment of magnetic moments, presented in figure 8(b). The latter inequality demands for the scalar products $\langle \mathbf{m}_i, \mathbf{r}_{ii+1} \rangle$, $\langle \mathbf{m}_i, \mathbf{r}_{ii+1} \rangle$ to have the same sign, which means that the angles between $\mathbf{m}_{i(i+1)}$ and $\mathbf{r}_{ii+1}$ are either both acute, or both obtuse.

With the new cluster definition the free energy of a ferroparticle dimer in the absence of an external magnetic field might be written as follows:

$$\begin{aligned} q_0(ii+1) = \frac{6}{d_{ii+1}^3} \int_0^{R_c(ii+1)} r_{ii+1}^2 \, \mathrm{d}r_{ii+1} \int_0^{\pi} \sin(\theta_{ii+1}) \, \mathrm{d}\theta_{ii+1} \int_0^{\pi} \sin(\omega_{ii+1}) \, \mathrm{d}\omega_{ii+1} \\ \times \exp\left\{ \frac{\lambda_{ii+1} d_{ii+1}^3}{r_{ii+1}^3} \left[\cos(\omega_{ii+1})(1 - \cos^2(\theta_{ii+1})) \right] \right\} \\ \times \exp\left(-\frac{U_{LJ}(ii+1)}{kT} \right) I_0 \left(\frac{\lambda_{ii+1} d_{ii+1}^3}{r_{ii+1}^3} \cos(\theta_{ii+1}) \sin(\theta_{ii+1}) \sin(\omega_{ii+1}) \right), \end{aligned} \tag{16}$$

where $I_0(\cdot)$ designates the modified Bessel function of zero order. When the applied magnetic field is strong, and the magnetic moments of the ferroparticles are coaligned with the external

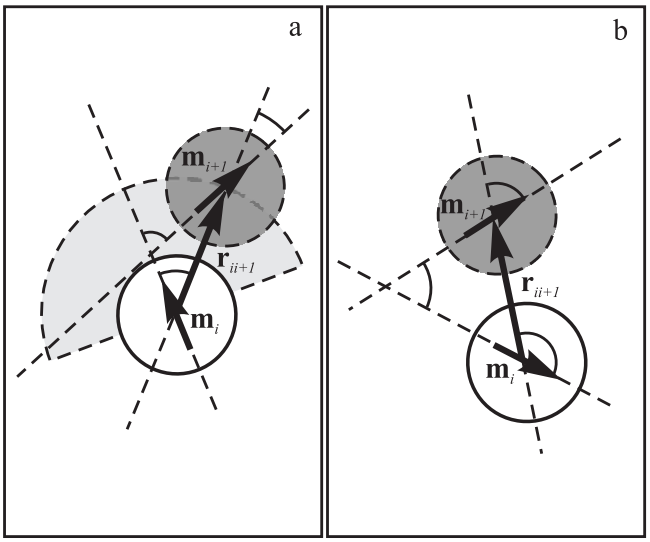

Figure 8. Illustration for the *entropic* cluster criterion. The sector shown in (a) in light grey describes the allowable region for the second particle. The radius of this sector is equal to the Lennard-Jones cutoff radius R_c. Marked angles $\mathbf{m}_i \hat{} \mathbf{m}_{i+1}$, $\mathbf{m}_i \hat{} \mathbf{r}_{ii+1}$, $\mathbf{m}_{i+1} \hat{} \mathbf{r}_{ii+1}$ are acute here; this means that all necessary scalar products are positive. Part (b) explains the necessity of the third item in the criterion. Two particles, which are not bound, are presented here. Nevertheless the distance is limited by R_c and the angle $\mathbf{m}_i \hat{} \mathbf{m}_{i+1}$ is acute, and the scalar products $\langle \mathbf{m}_i, \mathbf{r}_{ii+1} \rangle$, $\langle \mathbf{m}_{i+1}, \mathbf{r}_{ii+1} \rangle$ have different signs: $\langle \mathbf{m}_i, \mathbf{r}_{ii+1} \rangle < 0$, $\langle \mathbf{m}_{i+1}, \mathbf{r}_{ii+1} \rangle > 0$.

magnetic field, the expression (16) might be simplified:

$$q_\infty(ii+1) = \frac{12}{d_{ii+1}^3} \int_0^{R_c(ii+1)} r_{ii+1}^2 \, \mathrm{d}r_{ii+1} \int_0^\pi \sin(\theta_{ii+1}) \, \mathrm{d}\theta_{ii+1} \times \exp\left\{ \frac{\lambda_{ii+1} d_{ii+1}^3}{r_{ii+1}^3} \left[(1 - 3\cos^2(\theta_{ii+1})) \right] \right\} \exp\left(-\frac{U_{\mathrm{LJ}}(ii+1)}{kT} \right). \quad (17)$$

In regions of zero and infinitely intensive magnetic field the chain partition function $Q(i, n, m, 0(H_{\max}))$ can be presented in a form much easier than in expression (7), because factorization takes place:

$$Q(i, n, m, 0(H_{\max})) = q_{0(\infty)}^b(\mathrm{sl}) q_{0(\infty)}^c(\mathrm{ll}). \quad (18)$$

In order to check whether it is the criterion which is responsible for the deviations in cluster analysis, there is no necessity to generalize expression (18) for the arbitrary valued external magnetic field. In case the deviations vanish (remain) in two (or one of the) limiting cases this will be a positive (negative) confirmation. So, all theoretical microstructural observables were recalculated in zero and infinite external magnetic field with the new expression for the chain energy (18). The simulation data was reanalysed in accordance with the above-mentioned entropic criterion. Here an extensive comparison of the theoretical predictions to the newly obtained simulation results is carried out. The chain growth as a function of large particle concentration is presented in figure 9. Here the values of $N(0, \phi_l, 0.07 - \phi_l)$ (figure 9(a)) and $N(H_{\max}, \phi_l, 0.07 - \phi_l)$ (figure 9(b)) are plotted as functions of large particle concentration in a zero (figure 9(a)) and maximal (figure 9(b)) external field for the fixed total concentration $\phi = 0.07$. Here and in subsequent figures again dots correspond to the simulation data, solid curves describe theoretical results, and computational errors are presented by error bars. As is

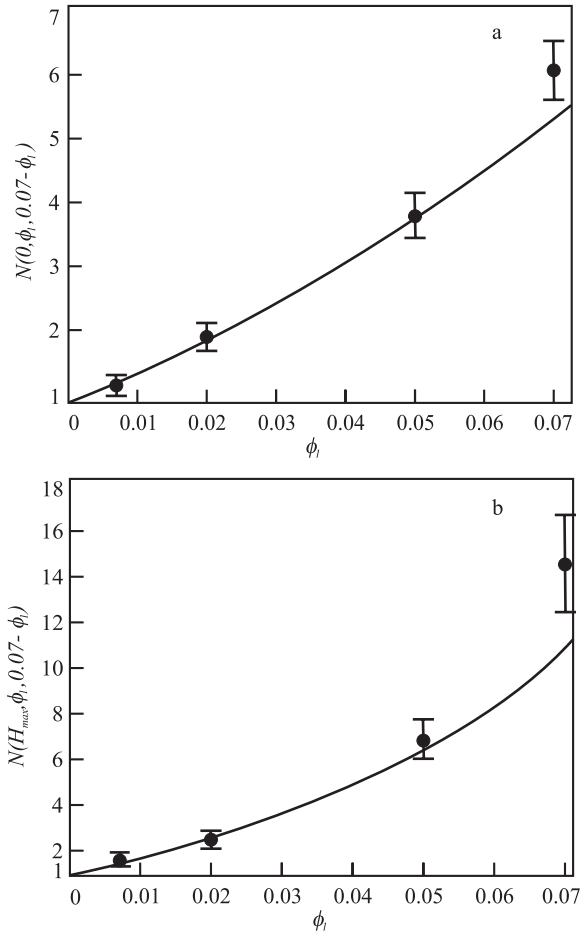

Figure 9. The chain growth as a function of large particle concentration. In (a) the value of $N(0, \phi_l, 0.07 - \phi_l)$ is plotted. In (b) the value $N(H_{\max}, \phi_l, 0.07 - \phi_l)$ is presented. In both (a) and (b) the total concentration is fixed at $\phi = 0.07$. Dots correspond to the simulation data, solid curves describe theoretical results, and computational errors are presented by error bars.

seen, both the qualitative and the quantitative behaviours are similar in theory and in computer simulations when the unified entropy criterion is used.

It is not only the mean chain length which characterizes the aggregated system. The number of such chains is also important in a cluster analysis. This information could be extracted from the number of large particles which take part in cluster formation. In terms of chain concentrations this observable is

$$S(H, \phi_l, \phi_s, n) = \frac{ng(i, n, m, H)}{\phi_l}. \tag{19}$$

In figures 10(a)–(d) the average number of large particles which take part in forming clusters, named $S(0, \phi_l, 0.07 - \phi_l, n)$, is presented versus the number of large particles n for different large particle concentration in the absence of an external magnetic field ($\phi = 0.07$). The analysis of these curves show that with the growth of small particle concentration (from $\phi_s = 0$ in figure 10(a), figure 10(b) $\phi_s = 0.02$, figure 10(c) $\phi_s = 0.05$ to $\phi_s = 0.063$ in figure 10(d)) the number of singlets increases sufficiently. In the monodisperse large particle system the

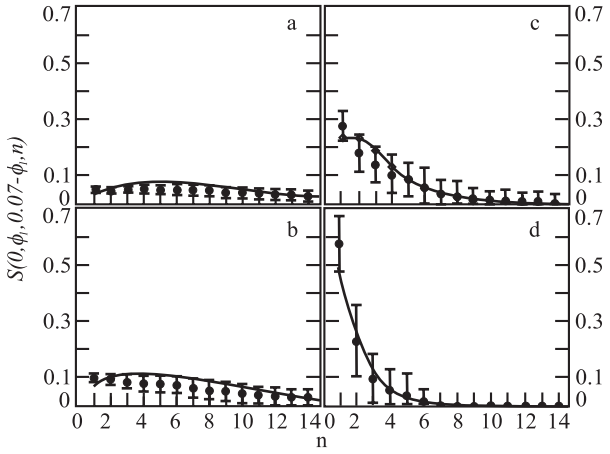

Figure 10. The average number of large particles which take part in forming clusters, named $S(0, \phi_l, 0.07 - \phi_l, n)$, versus the number of large particles n per chain for different large particle concentration in the absence of an external magnetic field: $\phi_s = 0$ (a), 0.02 (b), 0.05 (c), 0.063 (d). The total particle volume fraction ϕ is fixed at 0.07. Dots correspond to the simulation data, solid curves describe theoretical results, and computational errors are presented by error bars.

function $S(H, 0.07, 0, n)$ has a maximum at $n \sim 5$. This means that the majority of chains are composed by approximately five particles, which is in good agreement with mean chain length shown in figure 9(a) (the last point). When the concentration of small particles is equal to 0.063 almost all particles remain single and the curve $S(H, 0.007, 0.063, n)$ decreases monotonically to zero. The agreement between the computer simulation and the theoretical model might easily be called quantitative.

In the next part of this section the concentration of large particles is fixed at $\phi_l = 0.05$. In figures 11(a), (b) the chain length $N(H, 0.05, \phi_s)$ as a function of small particle concentration is presented for zero (figure 11(a), $N(0, 0.05, \phi_s)$) and infinite (figure 11(b), $N(H_{max}, 0.05, \phi_s)$) external magnetic field. Here dots stand for the simulation results and the theoretically obtained chain shortening is illustrated by a solid line; the vertical lines represent error bars of the numerical cluster analysis with the entropy criterion. This figure appears to be another example of quantitative coincidence between the theoretical results and simulation data with the same cluster definition.

In figures 12(a)–(d) the average number of large particles which take part in forming clusters, $S(H, 0.05, \phi_s, n)$, is presented versus the number of large particles n for different small particle concentration in the absence of an external magnetic field ($H = 0$, $\phi_l = 0.05$). The same function $S(H, 0.05, \phi_s, n)$, but for an infinite external magnetic field ($H = H_{max}$), is plotted in figures 13(a)–(d) ($\phi_l = 0.05$). In both sets of figures 12 and 13 plots 12(13)a correspond to the value of small particle concentration ϕ_s equal to $\phi_s = 0$, 12(13)b—to $\phi_s = 0.005$, in 12(13)c $\phi_s = 0.03$, and in 12(13)d the small particle concentration reaches the value $\phi_s = 0.05$. The tendency observed in these figures is close to the one discussed for figure 10. The larger the concentration of small particles is, the shorter are the chains. Under the influence of an external magnetic field no qualitative difference in the system behaviour is observed; only the maximum of $S(H, 0.05, \phi_s, n)$ is shifted to larger values of n, which means that the number of long chains increases. In both figures the theoretical curves fit into the simulation error bars.

In the last figure (figure 14) the average number of small particles per chain $N_s(0, 0.05, \phi_s)$ is given. It is plotted versus small particle concentration in the absence of an external

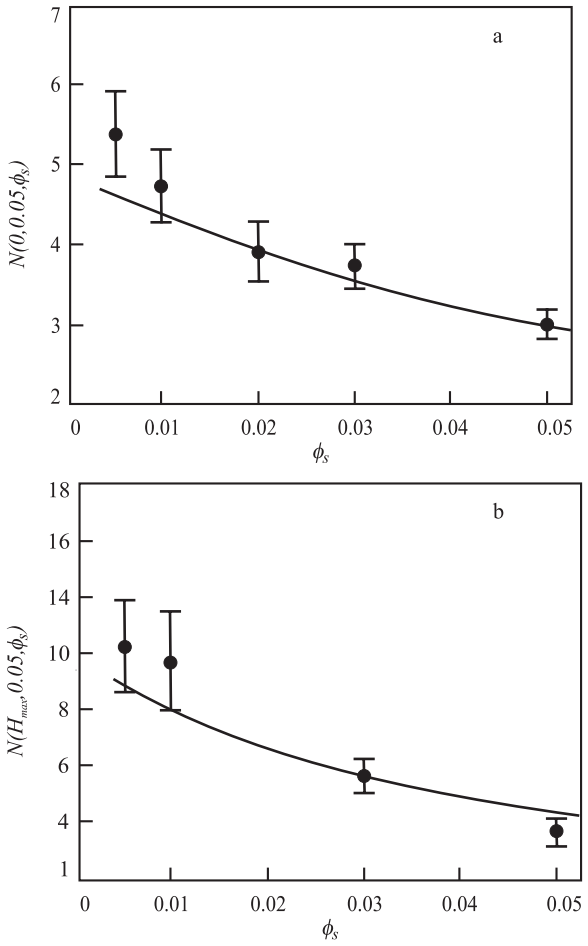

Figure 11. (a) Mean chain length $N(0, 0.05, \phi_s)$ as a function of small particle concentration for zero external magnetic field. (b) Mean chain length $N(H_{\max}, 0.05, \phi_s)$ as a function of small particle concentration for infinite external magnetic field. The concentration of large particles is fixed at $\phi_l = 0.05$. Dots stand for the simulation results and the theoretically obtained chain shortening is illustrated by a solid line; the vertical lines represent error bars of the numerical cluster analysis with the entropy criterion.

magnetic field. The comparison of the simulation data (dots) to the theoretical results (solid) is encouraging here.

Finally, the introduction of a new entropy cluster definition into both theory and simulations allowed us to obtain total quantitative agreement between simulation and theoretical microstructural observables. Another important conclusion is the following. The nearest neighbour limitation and the neglect of interchain interaction which are still present in the theory are compensating each other, because no visible deviations due their absence were found in the cluster analysis. Unfortunately it is worth saying that this entropy criterion is unacceptable in the theoretical description of ferrofluid macroscopic properties. The point is that according to this criterion even slightly correlated particles which occasionally appeared to be close to each other are treated as a new kinetic stable unit. So, the theoretical approach with the entropic cluster definition overestimates the chain length, and as a consequence, the

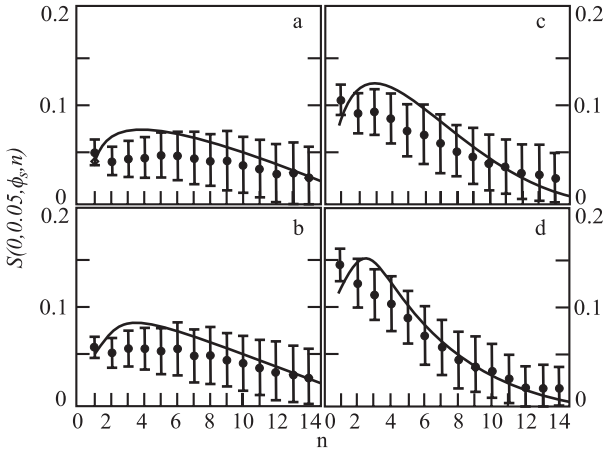

Figure 12. The average number of large particles which take part in forming clusters, $S(H, 0.05, \phi_s, n)$, versus the number of large particles n per chain for different small particle concentrations in the absence of an external magnetic field ($H = 0$, $\phi_l = 0.05$): $\phi_s = 0$ (a), 0.005 (b), 0.03 (c), 0.05 (d). Dots correspond to the simulation data, solid curves describe theoretical results, and the computational errors are presented by error bars.

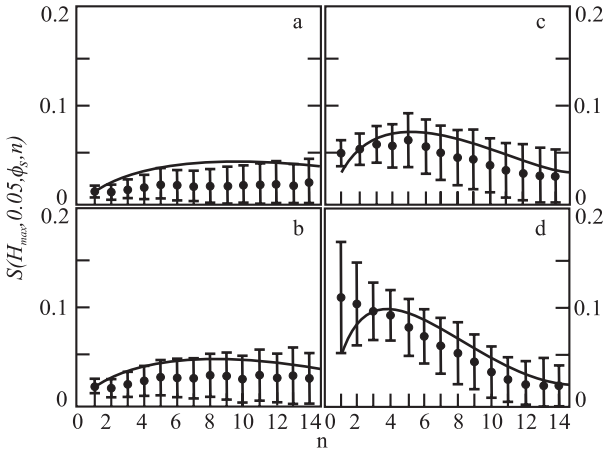

Figure 13. Function $S(H, 0.05, \phi_s, n)$ for an infinite external magnetic field versus the number of large particles n per chain for different small particle concentrations ($H = H_{max}$, $\phi_l = 0.05$): $\phi_s = 0$ (a), 0.005 (b), 0.03 (c), 0.05 (d). Dots correspond to the simulation data, solid curves describe theoretical results, and computational errors are presented by error bars.

influence of chains appears to be much stronger than in reality. Thus, the initial susceptibility calculated with this criterion is approximately twice as large as the observed one.

5. Conclusion

To summarize our theoretical achievements, we got rid of the major part of the approximations usually adopted in theoretical models devoted to the chain formation in ferrofluids. We treated a bidisperse model ferrofluid with flexible chains under the influence of an arbitrary valued external magnetic field theoretically and compared the results to the data obtained

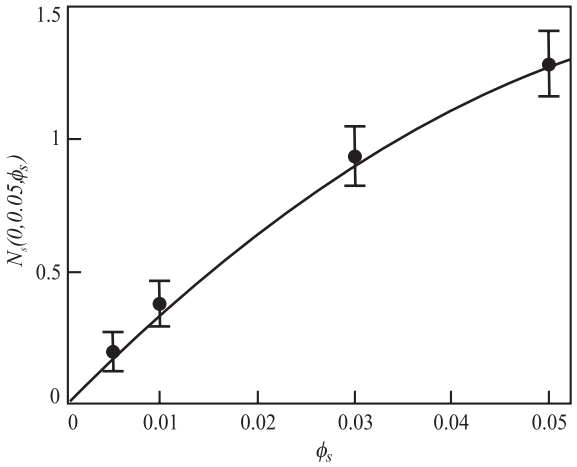

Figure 14. The average number of small particles per chain $N_s(0, 0.05, \phi_s)$ as a function of small particle concentration in zero external magnetic field. The concentration of large particles is fixed at $\phi_l = 0.05$. Dots correspond to the simulation data, the solid curve describes the theoretical results, and computational errors are presented by error bars.

via simulations of the fully interacting fluid. A novel theoretical approach was developed to describe the magnetostatic properties of a bidisperse model ferrofluid with chain aggregates. The chain partition function was calculated analytically allowing for the chain flexibility in an arbitrary valued external magnetic field. The presence of chains leads to an increase of the initial susceptibility in comparison with that of a homogeneous ferrocolloid. We were able to successfully describe this susceptibility growth which was found in computer simulations in binary model ferrocolloids with different granulometric compositions in terms of the developed approach. The chain flexibility which was taken into account in this approach allowed us to reach a convincing quantitative accord between theoretically and numerically obtained magnetization curves and the initial susceptibility for different granulometric compositions of a model fluid. However, a deeper analysis of the cluster structure showed noticeable deviations in cluster sizes and distributions. This occurs due to the use of different *energy* cluster criteria for the cluster analysis. The *energy* criterion used to analyse the simulations could not be used in the same way in the theoretical approach, and vice versa, due to technical problems. Nevertheless we found a convincing agreement between simulational and theoretical results for the qualitative (relative) behaviour of microstructural observables for various different model binary ferrofluids. This demonstrated that the deviations in cluster analysis were not qualitative, but were caused by the difference in the applied cluster criterion. To check this assertion we carried out an extensive theoretical and numerical cluster analysis using this time the same *entropic* cluster definition. This resulted in a full qualitative and quantitative agreement between simulation and theoretical microstructural observables. This also demonstrated that the nearest neighbour limitation and the neglect of interchain interaction which are still present in the theory are compensating each other in the region of investigated parameters of our systems. Unfortunately, the entropy criterion cannot be used for the theoretical description of ferrofluid macroscopic properties, because according to this criterion even slightly correlated particles which occasionally appeared to be close to each other are treated as a new kinetic stable unit, resulting in a large overestimation of the number of clusters, and as a consequence, this results in wrong macroscopic observables. However, one should keep in mind that an analysis of entropic chains is still valuable, since they are those very chains which are visible in

simulation snapshots and cryo-TEM images. As a result a natural question arises: 'What kind of chains should be taken into account?' Our presented results suggest that the chain definition has to be chosen according to the phenomena one wants to describe. Even if the snapshots or cryo-TEM images show the presence of chains in a system, this is not a reason to conclude that all of those chains are kinetically stable and correlated enough to influence the macroscopic properties of the investigated ferrocolloid.

Acknowledgments

The research was carried out with the financial support of INTAS Grant No 03-51-6064, RFBR Grant No 04-02-16078, CRDF Award No REC-005 and DFG Grant No HO 1108/8-4. One of the authors (SK) is grateful to the Dynasty Foundation and is supported by President RF Grant MK-4836.2006.2 and CRDF Grant Y3-P-05-11. We thank Z Wang for his help in analysing the simulation data.

References

[1] Resler E L and Rosensweig R 1964 *AIAA J.* **2** 1418
[2] Alexiou Ch, Jurgons R, Schmid R, Bergmann C, Henke J, Huenges E and Parak F 2003 *J. Drug Target* **11** 139
[3] Hilger I, Andrä W, Hergt R, Hiergeist R and Kaiser W A 2004 *Inorganic Materials, Recent Advances* ed D Bahadur, S Vitta and O Prakash (New Delhi: Narosa Publishing House)
[4] Shliomis M I 1974 *Usp. Fiz. Nauk* **112** 437
[5] Cebers A 1982 *Magnetohydrodynamics* **2** 42
[6] Pshenichnikov A F 1995 *J. Magn. Magn. Mater.* **145** 319
[7] Ivanov A O and Kuznetsova O B 2001 *Phys. Rev.* E **64** 041405
[8] Buyevich Y A and Ivanov A O 1992 *Physica* A **190** 276
[9] Taketomi S 1983 *Japan. J. Appl. Phys.* 1 **1137** 22
[10] Rasa M 1999 *J. Magn. Magn. Mater.* **201** 170
[11] Hasmoney E, Depeyrot J, Sousa M H, Tourinho F A, Bacri J C, Perzinski R, Raykher Yu L and Rosenman I 2000 *J. Appl. Phys.* **88** 6628
[12] Odenbach S and Gilly H 1996 *J. Magn. Magn. Mater.* **152** 123
[13] Odenbach S and Stork H 1998 *J. Magn. Magn. Mater.* **183** 188
[14] Odenbach S 2002 *Magnetoviscous Effects in Ferrofluids* (*Springer Lecture Notes in Physics*) (Berlin: Springer)
[15] Buzmakov V M and Pshenichnikov A F 1996 *J. Colloid Interface Sci.* **182** 63
[16] Wang Z and Holm C 2003 *Phys. Rev.* E **68** 041401
[17] Wang Z, Holm C and Müller H W 2002 *Phys. Rev.* E **66** 021405
[18] Camp Ph J and Patey G N 2000 *Phys. Rev.* E **62** 5403
[19] Pshenichnikov A F and Mekhonoshin V 2000 *J. Magn. Magn. Mater.* **213** 357
[20] Kruse T, Spanoudaki A and Pelster R 2003 *Phys. Rev.* B **68** 054208
[21] Klokkenburg M, Dullens R P A, Kegel W K, Erné B H and Philipse A P 2006 *Phys. Rev.* L **96** 037203
[22] Zubarev A Yu and Iskakova L Yu 1995 *J. Exp. Theor. Phys.* **80** 857
[23] Osipov M A, Teixeira P I C and Telo da Gama M M 1996 *Phys. Rev.* E **54** 2597
[24] Morozov K I and Shliomis M I 2002 *Ferrofluids, Magnetically Controllable Fluids and Their Applications* (*Springer Leacture Notes in Physics*) ed S Odenbach (Berlin: Springer)
[25] de Leeuw S W, Perram J W and Smith E R 1980 *Proc. R. Soc.* A **373** 27
[26] Allen M P and Tildesley D J 1987 *Computer Simulation of Liquids* (Oxford: Clarendon)
[27] Wang Z and Holm C 2001 *J. Chem. Phys.* **115** 6351
[28] Wang Z, Holm C and Müller H W 2003 *J. Chem. Phys.* **119** 379
[29] Huang J P, Wang Z and Holm C 2005 *Phys. Rev.* E **71** 061203
[30] Ivanov A O and Kantorovich S S 2004 *Phys. Rev.* E **70** 021401
[31] Frenkel' Ya I 1955 *Kinetic Theory of Liquids* (New York: Dover)
[32] Mendelev V S and Ivanov A O 2004 *Phys. Rev.* E **70** 051502
[33] Jordan P 1973 *Mol. Phys.* **25** 961
[34] Ivanov A O, Kantorovich S S, Mendelev V S and Pyanzina E S 2006 *J. Magn. Magn. Mater.* **300** 206